Hyperfine Interact
DOI 10.1007/s10751-010-0215-2

Mössbauer study of ^{57}Fe in GaAs and GaP following $^{57}Mn^{+}$ implantation

H. Masenda · D. Naidoo · K. Bharuth-Ram · H. P. Gunnlaugsson · G. Weyer · W. B. Dlamini · R. Mantovan · R. Sielemann · M. Fanciulli · T. E. Mølholt · S. Ólafsson · G. Langouche · K. Johnston · the ISOLDE Collaboration

© Springer Science+Business Media B.V. 2010

Abstract Ion implantation provides a precise method of incorporating dopant atoms in semiconductors, provided lattice damage due to the implantation process

H. Masenda (✉) · D. Naidoo
School of Physics, University of the Witwatersrand, Private Bag 3,
Johannesburg, WITS 2050, South Africa
e-mail: hilary.masenda@physics.org

D. Naidoo
DST/NRF Centre of Excellence in Strong Materials, University of the Witwatersrand,
Johannesburg, WITS 2050, South Africa

K. Bharuth-Ram · W. B. Dlamini
School of Physics, University of KwaZulu-Natal, Durban 4001, South Africa

H. P. Gunnlaugsson · G. Weyer ·
Department of Physics and Astronomy, Aarhus University,
Ny Munkegade 120, 8000 Århus C, Denmark

R. Mantovan · M. Fanciulli
Laboratorio MDM CNR-IMM, Via C. Olivetti 2, 20041 Agrate Brianza (MB), Italy

R. Sielemann
Helmholtz-Zentrum Berlin für Materialien und Energie, 14109 Berlin, Germany

M. Fanciulli
Dipartimento di Scienza dei Materiali, Università di Milano Bicocca, Via R. Cozzi 53,
20125 Milano, Italy

T. E. Mølholt · S. Ólafsson
Science Institute, University of Iceland, Dunhaga 3, 107 Reykjavik, Iceland

G. Langouche
Instituut voor Kern- en Stralingsfysica, University of Leuven, 3001 Leuven, Belgium

K. Johnston · the ISOLDE Collaboration
EP Division, CERN, 1211 Geneva 23, Switzerland

Published online: 23 November 2010

can be annealed and the dopant atoms located on regular lattice sites. We have undertaken ^{57}Fe emission Mössbauer spectroscopy measurements on GaAs and GaP single crystals following implantation of radioactive $^{57}Mn^{+}$ ions, to study the lattice sites of the implanted ions, the annealing of implantation induced damage and impurity–vacancy complexes formed. The Mössbauer spectra were analyzed with four spectral components: an asymmetric doublet (D1) attributed to Fe atoms in distorted environments due to implantation damage, two single lines, S1 assigned to Fe on substitutional Ga sites, and S2 to Fe on interstitial sites, and a low intensity symmetric doublet (D2) assigned to impurity–vacancy complexes. The variations in the extracted hyperfine parameters of D1 for both materials at high temperatures ($T > 400$ K) suggests changes in the immediate environment of the Fe impurity atoms and different bonding mechanism to the Mössbauer probe atom. The results show that the annealing of the radiation induced damage is more prominent in GaAs compared to GaP.

Keywords Emission Mössbauer spectroscopy · ^{57}Fe · ^{57}Mn · GaAs · GaP

1 Introduction

Impurity defects in semiconductors have been an area of interest over the past few decades, stimulated by the growing importance of semiconductors in high-frequency and optoelectronic devices [1, 2]. The incorporation of extrinsic defects in semiconductors by ion implantation and appropriate annealing gives rise to instabilities that profoundly affect their electronic and optical properties. Consequently, the knowledge of the annealing behavior of the implantation induced damage, site location of the implanted atoms and hence the chemical nature of these defects is vital for the understanding of new properties in doped compound semiconductors. Hyperfine interaction methods, in particular Mössbauer spectroscopy is a powerful technique to investigate impurities in semiconductors, giving information on the electronic configuration of the impurity ions and their site symmetry.

Previous Mössbauer studies of Sn impurity atoms in GaAs [3–5] and GaP [6, 7] and other group III–V semiconductors such as InP, InAs, and InSb [8–11] using implantation of radioactive ^{119}In and ^{119m}Sn as precursor isotopes have shown that $\sim 60\%$ Sn atoms occupy substitutional III sites upon implantation and thermal annealing at temperatures above 625 K [6]. However, ^{119}Sb implantations [12] showed Sb on substitutional V sites that dominated after annealing at 350°C. These sites were then inherited by the ^{119}Sn Mössbauer daughter atoms which maintained the respective lattice locations due to the lower recoil energies imparted to the Sn atoms compared to the displacement threshold energies. Site selective implantation [8] was observed for different types of precursor isotopes which decayed to ^{119}Sn in the 24 keV Mössbauer state. As an amphoteric dopant, Sn atoms that occupied substitutional III or V sites act as a donor or an acceptor, respectively [11]. Mössbauer emission spectroscopy studies of Fe impurities in GaAs after implantation of radioactive ^{57}Co (^{57m}Fe) [13] showed that the Fe atoms were located in a disordered environment and after annealing of the implantation damage between 300–450°C, a single line was observed in the spectra.

In the present study, results from ^{57}Fe Mössbauer emission spectroscopy experiments following implantation of radioactive ^{57}Mn$^+$ atoms in GaP and GaAs are reported.

2 Experimental details and data analysis

Radioactive ion beam of ^{57}Mn* ($T_{1/2} = 1.5$ min) is produced at the ISOLDE facility at CERN, using a 1.4 GeV proton-induced nuclear fission in a UC_2 target. The ^{57}Mn atoms are subsequently ionized by multi-frequency, element specific, laser irradiation and then accelerated to an energy of 60 keV before they are magnetically mass separated to yield a pure beam of $\sim$ (1–3)$\times 10^8$ ^{57}Mn$^+$/s [14]. The GaAs and GaP single crystals were held at temperatures between 77–700 K and implanted with ^{57}Mn$^+$ ions with low fluence ($<10^{12}$/cm^2) to avoid overlapping damage cascades. ^{57}Mn* β^- decays to the 14.4 keV Mössbauer state of ^{57m}Fe ($T_{1/2} = 98$ ns). Mössbauer spectra were recorded with an acetone gas-filled resonance detector equipped with ^{57}Fe enriched stainless steel foils mounted on a conventional velocity drive system outside the implantation chamber. The detector was mounted 90° to the beam direction and 60° relative to the crystal surface normal. The velocity and isomer shift values are calibrated relative to α-Fe at room temperature.

3 Results and discussion

The Mössbauer spectra obtained for GaAs and GaP, together with fitted spectral components, are shown in Fig. 1 as a function of temperature. The fits were performed in an iterative procedure taking advantage of the temperature dependent appearance or disappearance of spectral components for their unequivocal identification. Simultaneous analysis of all spectra required four spectral components: (i) an asymmetrically broadened doublet (D1), (ii) a single line (S1), (iii) a symmetric doublet (D2) present over the measured temperature range, and (iv) a single line (S2) with low intensity only present below 320 K. The total area of all components closely followed the Debye model temperature dependence behavior, justifying the assumption that the spectral area fraction of each component represents its respective state or site population to a good approximation, with minor corrections at the highest measured temperatures.

The isomer shift (δ) and quadrupole splitting (ΔE_Q) values of all components with the exception of D1 were restricted to follow the second order Doppler shift (SOD) and $T^{3/2}$ dependence [15], respectively, over the measured temperature range. The Gaussian broadening of D1 was found to decrease at increasing temperature, and in the final analysis it was constrained to follow a smooth decrease. The extracted hyperfine parameters of all spectral components for both materials are presented in Table 1.

The asymmetry of the doublet D1 is similar to the components observed in group IV semiconductors after ^{57}Mn$^+$ implantation [15–18] assigned to Fe in isolated disordered regions. The broad line-width coupled with the asymmetry of this component results from correlated distribution of the isomer shift and quadrupole

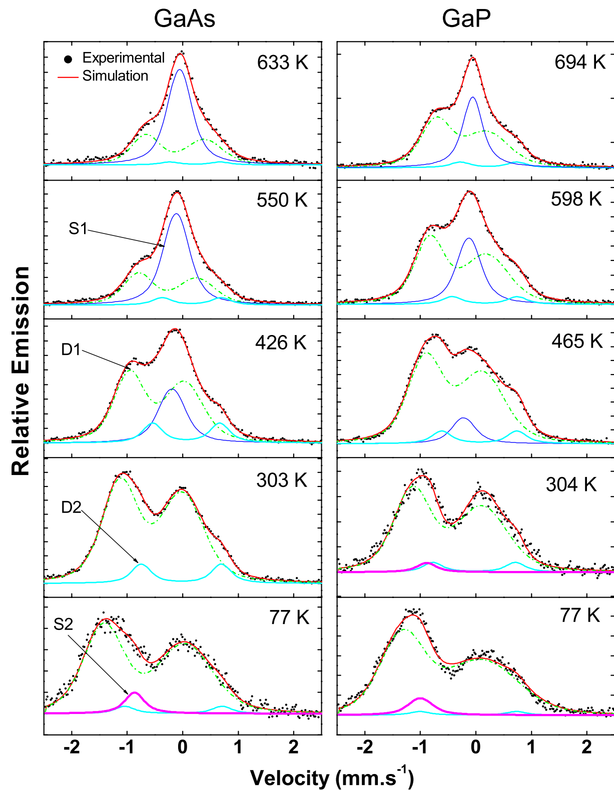

Fig. 1 Selected ^{57}Fe Mössbauer spectra obtained after implantation for $^{57}Mn^{+}$ in GaAs and GaP, at the temperatures indicated

Table 1 Extracted hyperfine parameters of the various spectral components obtained at room temperature for GaAs and GaP

($mm.s^{-1}$)	D1		D2		S1	S2
	δ	ΔE_Q	δ	ΔE_Q	δ	δ
GaAs	0.57 (4)	1.12 (2)	0.02 (2)	1.43 (3)	0.29 (4)	0.99 (2)[a]
GaP	0.51 (5)	1.25 (4)	0.04 (5)	1.48 (1)	0.34 (2)	1.03 (3)[a]

[a]Isomer shift at 77 K

splitting of Fe impurity sites [17], most probably as a consequence of the Mössbauer probe atoms being located in isolated amorphous regions. Such spatially isolated disordered zones [19] have been observed by transmission electron microscopy in GaP and GaAs after 50 keV Xe^{+} implantation with fluences $\leq 2 \times 10^{11}$ ion/cm^2. D1 is assigned to Fe atoms in implantation related damage sites (Fe_D). The damage site shows marked annealing stages of 300–600 K for GaP and 300–550 K for GaAs, which leads to a corresponding increase in the intensity of the single line S1 in both materials. Component S1 is assigned to substitutional Fe at Ga sites. This assignment is consistent with Mössbauer measurements of ^{119}Sn implanted into GaAs where the observed spectra at high temperature implantations (525–625 K) were dominated by a single line assigned to Sn on substitutional Ga sites [5–7]. The absence of S1 at temperatures below 320 K is due to the fact that Fe at this site forms upon annealing

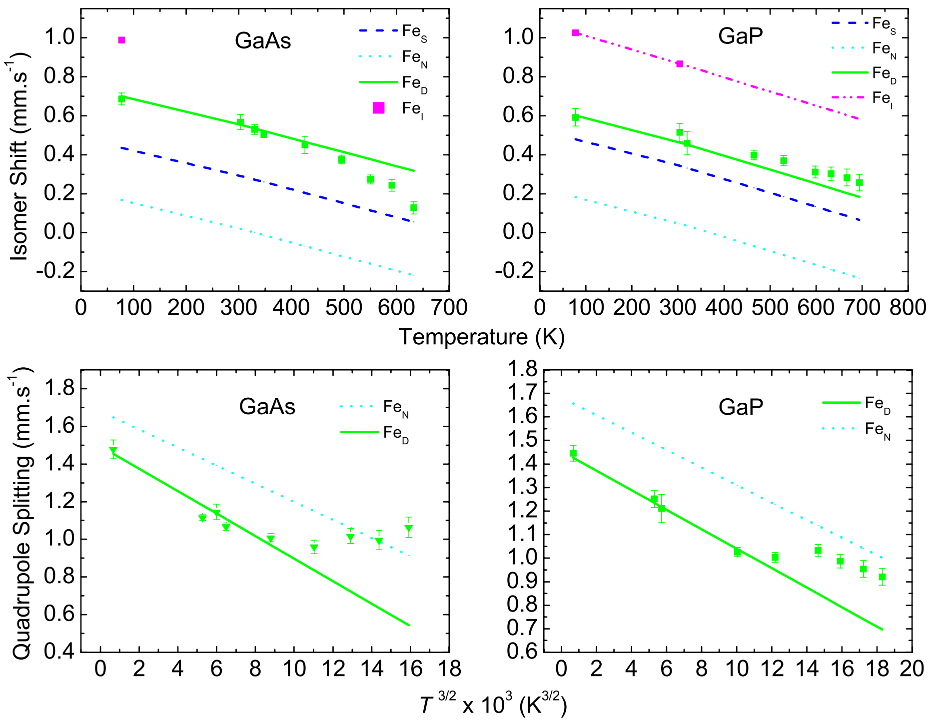

Fig. 2 Temperature dependence of the isomer shift and quadrupole splitting values observed in Mössbauer spectra for GaAs and GaP after ^{57}Mn^{+} implantation

of the lattice damage. A higher isomer shift of Fe$_D$($\delta_{D,GaAs}$ = 0.57(4) mm.s^{-1}, $\delta_{D,GaP}$ = 0.51(5) mm.s^{-1}) corresponds to a decrease in the electron density at the nucleus relative to the Fe$_S$ component ($\delta_{S,GaAs}$ = 0.29(4) mm.s^{-1}, $\delta_{S,GaP}$ = 0.34(2) mm.s^{-1}) which suggests some relaxation of the lattice surrounding the amorphous pockets. An even lower electron density is characteristic of the single line S2 ($\delta_{I,GaAs}$ = 0.99(2) mm.s^{-1}, $\delta_{I,GaP}$ = 1.03(3) mm.s^{-1}) relative to Fe$_S$ is indicative of Fe impurity atoms located in interstitial positions (Fe$_I$) without bonding to nearest neighbor atoms. A very high electron density coupled with high loss of symmetry at the nucleus of the Mössbauer probe with respect to S1 is associated with component D2. In GaAs, this component shows a decrease in the site population around 600 K and a corresponding increase in the area fraction of the substitutional line suggests that this component may be related to impurity–vacancy complexes (Fe$_N$). Similar complexes have been observed in Mössbauer investigations on Sn implanted GaAs [6, 7].

At temperatures below 400 K, the isomer shift and quadrupole splitting values of Fe$_D$ follow the second order Doppler shift and $T^{3/2}$ dependence, respectively as shown in Fig. 2. However, in GaAs, the isomer-shift values are lower than the SOD trend from lower temperature behavior and the extracted isomer shift values in GaP were higher than the SOD prediction above 400 K. In this study the observed annealing stage in GaP (300–600 K) is in agreement with positron annihilation studies [20–23] where annealing of Ga vacancies is observed. Similar positron lifetime

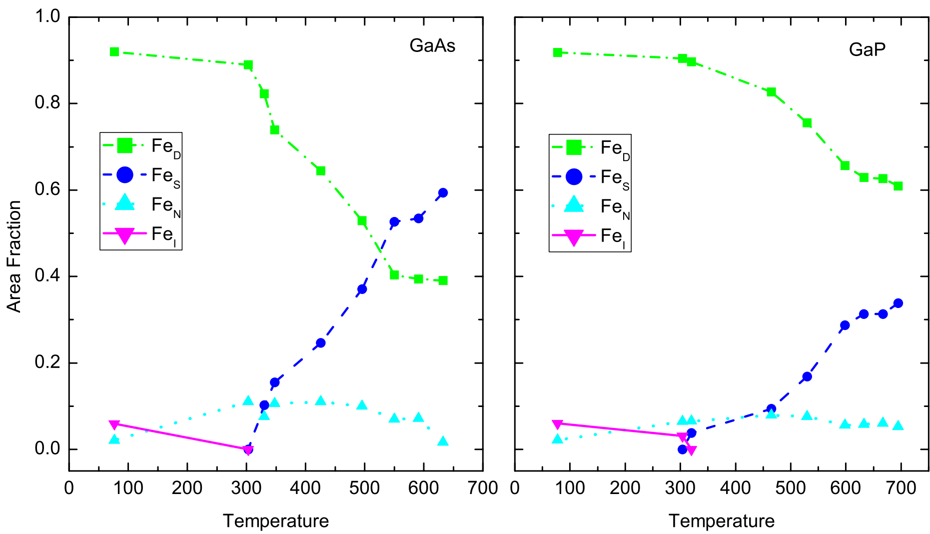

Fig. 3 Comparison of area fractions of the different spectral components as a function of temperature in GaP and GaAs

Table 2 Average Debye temperatures of Fe in GaAs and GaP

Material	Site	θ_D^{av} (K)	θ_D^{MDA} (K)
GaP	Ga	283 (9)	347
	P		315
GaAs	Ga	259 (8)	309
	As		297

investigations in GaAs [24] within our observed annealing stage (300–550 K) suggest the recombination of vacancy-interstitial close pairs in the As sublattice in addition to the recovery of V_{Ga} [25, 26]. The difference in hyperfine parameters at high temperatures with respect to the expected SOD for δ and $T^{3/2}$ dependence of ΔE_Q, based on low temperature measurements could be associated with changes in the surrounding and impurity-defect bonding mechanism of the Mössbauer probe nucleus in small amorphous zones associated with more extended defects created above 400 K.

Different annealing behaviors of the implantation induced damage are evident in GaAs and GaP, resulting in a significant increase in the Fe_S site population. The recovery of the damage is more prominent in GaAs than in GaP as depicted in the plot of areal fractions in Fig. 3.

The average Debye temperatures $\left(\theta_D^{av}\right)$ of Fe in both GaP and GaAs (see Table 2) were calculated after satisfactory simultaneous analyses where the area fractions were assumed to follow a Debye behavior. The obtained average Debye temperatures are comparable with the theoretical values predicted by the mass-defect approximation $\left(\theta_D^{MDA}\right)$ using the host atom Debye temperatures obtained from *B*-factors i.e. theoretical Debye-Waller factors for both sublattices calculated by Reid [27]. The higher average Debye temperatures and theoretically calculated values for the different sublattices in GaP compared to GaAs suggests that Fe-P

bonds are stronger than the Fe-As bonds in respective materials. In addition, minor variations in the site population of Fe_N which is assigned to Fe_{In}-V_{In} complexes are observed over the measured temperature. This component is more stable in GaP compared to GaAs at temperatures >300 K as reflected by an approximately constant area fraction while a small decrease is observed in GaAs at the highest measured temperature.

4 Conclusions

Our measurements have shown that Fe atoms in both GaP and GaAs single crystals are located: (i) on substitutional Ga sites (Fe_{Ga}); (ii) in interstitial sites; (iii) in impurity–vacancy complexes; (iv) in distorted environments (damage). The lattice damage does not anneal completely at the highest measured temperatures of our measurements. This may be due to the creation of more extended Fe-defect complexes. The increase in the quadrupole splitting of Fe_D suggests changes in the immediate environment of the Mössbauer probe nucleus while different Fe-defect bonding mechanisms in both materials are predictable from the different isomer shift trends with respect to the expected second-order Doppler shift based on low temperature data. The slower recovery of the radiation damage and higher average Debye temperature in GaP than in GaAs shows that Fe forms stronger bonds in GaP compared to GaAs.

Acknowledgements This work was supported by the European Union Sixth Framework through RII3-EURONS. K. Bharuth-Ram, W.B. Dlamini, H. Masenda and D. Naidoo acknowledge support from the South African National Research Foundation. T. E. Mølholt acknowledges support from the Icelandic Research Fund.

References

1. Bosi, M., Pelosi, C.: Prog. Photovolt: Res. Appl. **15**, 51–68 (2007)
2. Queisser, H.J., Halle, E.E.: Science **281**, 945–946 (1998)
3. Holm, N.E., Nylandsted, A., Deutch, B.I., Weyer, G.: Inst. Phys. Conf. Ser. No. **46**, 735 (1979)
4. Weyer, G., Damgaard, S., Petersen, J.W., Heinemeier, J.: Phys. Stat. Sol. (B) **98**, K147 (1980)
5. Weyer, G., Petersen, J.W., Damgaard, S.: Hyp. Int. **15/16**, 495–498 (1983)
6. Holm, N.E., Weyer, G.: J. Phys. Chem: Solid State Phys. **13**, 1109–1120 (1980)
7. Weyer, G., Damgaard, S., Petersen, J.W., Heinemeier, J.: J. Phys. Chem: Solid State Phys. **13**, L181–L183 (1980)
8. Weyer, G., Petersen, J.W., Damgaard, S., Nielsen, H.L., Heinemeier, J.: Phys. Rev. Lett. **44**, 155–157 (1980)
9. Weyer, G., Petersen, J.W., Damgaard, S.: Physica **116B**, 470–473 (1983)
10. Nielsen, O.H., Larsen, F.K., Damgaard, S., Petersen, J.W., Weyer, G.: Z. Phys. B **52**, 99–109 (1983)
11. Weyer, G., Petersen, J.W., Damgaard, S.: Physica **117B & 118B**, 523–525 (1983)
12. Weyer, G., and the ISOLDE Collaboration: Hyp. Int. **129**, 371–390 (2000)
13. Schroyen, D., Dezsi*, I., Langouche, G.: Hyp. Int. **29**, 1255–1258 (1986)
14. Fedoseyev, V.N., Bätzner, K., Catherall, R., Evens, A.H.M., Forkel-Wirth, D., Jonsson, O.C., Kugler, E., Lettry, J., Mishin, V.I., Ravn, H.L., Weyer, G., and the ISOLDE Collaboration: Nucl. Instrum. Methods B **126**, 88 (1997)
15. Gunnlaugsson, H.P., Bharuth-Ram, K., Dietrich, M., Fanciulli, M., Fynbo, H.O.U., Weyer, G.: Hyp. Int. **169**, 1319–1323 (2006)
16. Gunnlaugsson, H.P., Fanciulli, M., Dietrich, M., Baruth-Ram, K., Sielemann, R., Weyer, G., the ISOLDE collaboration: Nucl. Instrum. Methods B **168**, 55–60 (2002)

17. Weyer, G., Gunnlaugsson, H.P., Dietrich, M., Fanciulli, M., Baruth-Ram, K., Sielemann, R., and the ISOLDE collaboration: Nucl. Instrum. Methods B **206**, 90–94 (2003)
18. Weyer, G., Gunnlaugsson, H.P., Dietrich, M., Fynbo, H., Bharuth-Ram, K., and the ISOLDE Collaboration: Eur. Phys. J.–Appl. Phys. **27**, 317–320 (2004)
19. Jencic, I., Bench, M.W., Robertson, I.M., Kirk, M.A.: J. Appl. Phys. **78**(2), 972–984 (1995)
20. Gupta, A.S., Moser, P., Corbel, C., Hautojärvi, P., Sen, P.: Cryst. Res. Technol. **23**, 243–246 (1988)
21. Gupta, A.S.: Bull. Mater. Sci. **13**, 89–94 (1990)
22. Dlubek, G., Ascheron, C., Krause, R., Erhard, H., Klimm, D.: Phys. Stat. Sol. (A) **106**, 81–88 (1988)
23. Polity, A., Abgarjan, T.h., Krause-Rehberg, R.: Appl. Phys. **A60**, 541–544 (1995)
24. Pons, D.: Physica B **116**, 388–393 (1983)
25. Itoh, Y., Murakami, H.: Appl. Phys. **A58**, 59–62 (1994)
26. Corbel, C., Pierre, F., Saarinen, K., Hautojärvi, P., Moser, P.: Phys. Rev B **45**, 3386–3399 (1992)
27. Reid, J.S.: Acta Cryst. **A39**, 1–13 (1983)